

# Estimation of Molar Absorption Coefficients of HbA1c in Near UV-Vis-SW NIR Light Spectrum

Shifat Hossain\*, Tae-Ho Kwon\*, Ki-Doo Kim<sup>o</sup>

## ABSTRACT

Diabetes is a serious group of diseases that can cause many complicated problems including sudden mortality. Glycated hemoglobin tests are considered as a reliable tool to diagnose diabetes. To estimate amount of glycated hemoglobin (HbA1c) present in Red Blood Cells (RBCs) optically, the molar absorption coefficient of HbA1c is necessary. We calculate the molar absorption coefficient of HbA1c from percent transmittance spectrum of HbA1c dissolved in water and calibrate the values for a range with molar absorption coefficients of glycated hemoglobin at 535nm Green light and 593nm Yellow light references. We estimate the molar absorption coefficient in the range of 300nm to 1100nm, and we have got a characteristic peak of HbA1c at 411nm ( $5.20 \times 10^5 \pm 1.39 \times 10^5 \text{ M}^{-1} \text{ cm}^{-1}$ ) and two more peaks at 540nm ( $5.63 \times 10^5 \pm 1.51 \times 10^5 \text{ M}^{-1} \text{ cm}^{-1}$ ) and 576nm ( $4.96 \times 10^5 \pm 1.33 \times 10^5 \text{ M}^{-1} \text{ cm}^{-1}$ ), respectively. The characteristic and secondary peaks found in our study are verified with previous studies and found consistent with them. The calculated molar absorption coefficient from Near UV to shortwave NIR range can enable the way of non-invasive estimation of HbA1c.

**Key Words** : Molar absorption coefficient, glycated hemoglobin, HbA1c, absorption spectrum, percent transmission

## 1. Introduction

In general, diabetes mellitus is a chronic group of diseases. These refer to the abnormal usage of blood sugar in human body<sup>[1]</sup>. In 2014, around 422 million people all around the world was affected by this deadly disease<sup>[2]</sup>. There are two types of diabetes - type 1 diabetes and type 2 diabetes. Both of them results in building up of sugar in the bloodstream. Severe diabetes patients also prone to Cardiovascular diseases<sup>[3]</sup>, Nerve damage<sup>[4]</sup>, Eye damage<sup>[5]</sup>, bacterial and fungal infections of skin and respiratory system<sup>[6,7]</sup>,

Kidney damage<sup>[8]</sup> as well as Alzheimer's disease<sup>[9]</sup>. So, frequent monitoring of diabetes patients is necessary to control blood sugar level. Apart from the chronic group, there are also two potentially reversible diabetes conditions - prediabetes and gestational diabetes.

To diagnose diabetes, random blood sugar test, fasting blood sugar test and oral glucose tolerance tests are used medically<sup>[10-12]</sup>. All of these methods use blood sample to estimate the glucose amount in blood. Commonly available glucose measuring systems are mostly based on electrochemical sensors. These sensors are usually

\* This research was supported by Basic Science Research Program through the National Research Foundation (NRF) of Korea funded by the Ministry of Education (NRF-2019R1F1A1062317).

\* also supported by the National Research Foundation of Korea Grant funded by the Ministry of Science, ICT, and Future Planning [2015R1A5A7037615].

• First Author : Kookmin University Department of Electronics Engineering, shifathosn@kookmin.ac.kr, 정희원

◦ Corresponding Author : Kookmin University Department of Electronics Engineering, kdk@kookmin.ac.kr, 종신희원

\* Kookmin University Department of Electronics Engineering, kmjkh@kookmin.ac.kr, 학생희원

논문번호 : 2021-01-015-C-RN, Received January 14, 2021; Revised March 20, 2021; Accepted March 31, 2021

enzymatic and non-enzymatic and are highly accurate in terms of estimating blood glucose<sup>[13]</sup>. But finger pricking has some long-term disadvantages that includes tissue damage, recursive pain and increased risk of infection formation. Similarly, invasive continuous blood glucose monitors are inserted into subcutaneous tissue for getting close to the interstitial fluid (ISF). These types of sensors are also prone to errors due to movement and environmental noise caused by the Tx-Rx system and for the wireless data transmission mechanism.

Recently non-invasive techniques are emerging as an alternative to invasive methods to estimate glucose in a blood stream<sup>[14]</sup>. Among these technologies, bodily fluids (i.e. saliva, sweat, breath etc.), and tissues (i.e. skin) are used with painless contact sensors for glucose estimation<sup>[15]</sup>. Another form of non-invasive technology is optical estimation of glucose in blood stream. But estimating glucose optically could not produce reliable results<sup>[16]</sup>.

In another method of diabetes diagnosis, estimation of HbA1c is performed<sup>[17]</sup>. When sugar is exposed for long terms in the blood stream, glycated hemoglobin (HbA1c) is formed. HbA1c formation is an irreversible process called Glycation. This glycated hemoglobin can be present in the blood for about 120 days (about 4 months), related to the average life-span of hemoglobin cells. It is important to note that Glucose level represents instantaneous blood sugar level, so there is a great difference between pre-meal and post-meal levels, whereas HbA1c represents an average blood sugar level for 3 to 4 months, and has no relation with meals or daily routine. For these reasons, HbA1c concentration can be an important marker of long-term average glucose availability in blood stream, which is a reliable tool in the diagnosis of diabetes.

As the amount of glycated hemoglobin in blood changes very slowly (in about 3 months' span), it is not prone to sudden change in the range of hours due to lifestyle changes or fasting. According to American Diabetic Association

(ADA), presence of HbA1c more than 6.5% among all total hemoglobin in blood stream is diagnosed as a diabetic patient<sup>[18]</sup>.

There are many methods of estimating HbA1c levels in blood stream. High performance liquid chromatography, capillary electrophoresis etc. are used for in-Lab experiments to estimate HbA1c levels. These techniques involve blood samples from the patients.

Among all these invasive methods, the high-performance liquid chromatography (HPLC) is considered the gold standard for HbA1c estimation. In this method, the blood sample is collected and pressurized through a column of absorbent material (e.g., silica, divinylbenzene, etc.). This column of absorbent material changes the motion of the individual components of the blood solution due to individual components' size, ionization state, and many other factors. This process enables the separation of individual components from a blood solution (in this case, HbA1c). After the column, a detector is placed to measure the presence and concentration of individual compounds in a solution in terms of "time to travel" and "area under curve".

In medical applications, Photoplethysmography (PPG) is an optical measurement method that can be obtained noninvasively<sup>[19,20]</sup>. To form a PPG waveform, optoelectronic components are required. These components contain a light source that illuminates the tissue (e.g., the skin) and a photodetector (PD) that measures variations in blood volume through a change in light intensity. PPG signals have been used to detect heart rate<sup>[21]</sup>, respiration rate<sup>[22]</sup>, and blood oxygenation<sup>[23,24]</sup> from the human body. In this paper, we focus on the estimation of the molar absorption coefficient of HbA1c for non-invasive optical estimation of HbA1c levels. This work is the detailed extension of our previous work in [25].

As photoplethysmographic signals are a direct result of the change in volume of blood, the signal can be utilized to measure the individual components of the blood solution consisting

HbA1c compounds. As we know, PPG signals are optical signals. So, reverse calculation of the optical interactions in a solution can be utilized to estimate the HbA1c level in a practical scenario. Estimation of molar absorption coefficient of HbA1c enables the possibility of calculating the optical interactions, hence calculating the HbA1c level.

Though, the molar absorption coefficient of HbA1c is required to estimate HbA1c in a non-invasive way with PPG signals, the HPLC method described before does not depend on this coefficient value. This is due to the HPLC method depends on the molecular structure and interactions of the individual components of the solution with the absorbent material. But in contrast with the PPG, the HPLC method does not depend on the optical interactions with the solution itself.

### 1.1 Estimation of HbA1c from PPG Signal

The method of estimation of HbA1c from PPG signal is based on [26], which is derived from Beer-Lambert law of light absorption. In a homogenous solution of different absorbents, the Beer-Lambert law<sup>[27]</sup> states that

$$A = \sum_{i=1}^N A_i = \sum_{i=1}^N \epsilon_i \times c_i \times d = -\log \left( \frac{I}{I_0} \right) \quad (1)$$

where  $A$  is the total absorption of the solution,  $N$  number of attenuating species,  $\epsilon$  is the molar absorption coefficient [ $Lmol^{-1}cm^{-1}$ ],  $c$  is the molar concentration of the attenuator [ $molL^{-1}$ ]. Now applying this (1) in the case of blood, letting blood as a homogenous mixture of different types of hemoglobin. The types of hemoglobin to consider in our case are HbO (Oxy-hemoglobin), HHb (Deoxy-hemoglobin) and HbA1c (Glycated hemoglobin). The HbA1c component considered in this study consists of 98% oxygenated and 2% deoxygenated variant of glycated hemoglobin.

Now first we have to define the percentage definition of HbA1c and SpO2.

$$\%HbA1c = \frac{c_{HbA1c}}{c_{HHb} + c_{HbO} + c_{HbA1c}} \times 100 \quad (2)$$

$$\%SpO2 = \frac{c_{HbO}}{c_{HHb} + c_{HbO}} \times 100\% \quad (3)$$

And from (1) we can write for the homogenous mixture of those hemoglobin cells

$$A = \epsilon_{HHb}(\lambda) \times c_{HHb} \times d + \epsilon_{HbO}(\lambda) \times c_{HbO} \times d + \epsilon_{HbA1c}(\lambda) \times c_{HbA1c} \times d$$

$$A = (\epsilon_{HHb}(\lambda) \times c_{HHb} + \epsilon_{HbO}(\lambda) \times c_{HbO} + \epsilon_{HbA1c}(\lambda) \times c_{HbA1c}) \times d \quad (4)$$

Now if the sample is measured from two distances and subtracted from each other, then the (4) becomes,

$$\delta A = (\epsilon_{HHb}(\lambda) \times c_{HHb} + \epsilon_{HbO}(\lambda) \times c_{HbO} + \epsilon_{HbA1c}(\lambda) \times c_{HbA1c}) \times \delta d \quad (5)$$

where,  $\delta d = d_1 - d_2$ ;  $\delta A = A_1 - A_2$

The  $d_1$  and  $d_2$  can be described as the optical path length at systolic and diastolic points, respectively. Now if the sample is measured with two different wavelengths as well as different lengths, (5) is modified as,

$$\delta A_{\lambda 1} = (\epsilon_{HHb} \times c_{HHb} + \epsilon_{HbO} \times c_{HbO} + \epsilon_{HbA1c} \times c_{HbA1c}) \times \delta d \quad (6)$$

$$\delta A_{\lambda 2} = (\epsilon_{HHb} \times c_{HHb} + \epsilon_{HbO} \times c_{HbO} + \epsilon_{HbA1c} \times c_{HbA1c}) \times \delta d \quad (7)$$

Now we define the ratio of these two equations as  $R$ .

$$R = \frac{\delta A_{\lambda 1}}{\delta A_{\lambda 2}} = \frac{\epsilon_{HHb}(\lambda_1) \times c_{HHb} + \epsilon_{HbO}(\lambda_1) \times c_{HbO} + \epsilon_{HbA1c}(\lambda_1) \times c_{HbA1c}}{\epsilon_{HHb}(\lambda_2) \times c_{HHb} + \epsilon_{HbO}(\lambda_2) \times c_{HbO} + \epsilon_{HbA1c}(\lambda_2) \times c_{HbA1c}} \quad (8)$$

The (2) and (3) can be rewritten as

$$c_{HbO} = \frac{\%SpO2}{100} \times (c_{HHb} + c_{HbO}) \quad (9)$$

$$c_{HHb} = \left(1 - \frac{\%SpO2}{100}\right) \times (c_{HHb} + c_{HbO}) \quad (10)$$

$$c_{HbA1c} = \frac{\%HbA1c}{100} \times (c_{HHb} + c_{HbO} + c_{HbA1c}) \quad (11)$$

$$c_{HHb} + c_{HbO} = \left(1 - \frac{\%HbA1c}{100}\right) \times (c_{HHb} + c_{HbO} + c_{HbA1c}) \quad (12)$$

Now (9) and (10) can be rewritten as

$$c_{HbO} = \frac{\%SpO_2}{100} \times \left(1 - \frac{\%HbA1c}{100}\right) \times (c_{HbB} + c_{HbO} + c_{HbA1c}) \quad (13)$$

$$c_{HbB} = \left(1 - \frac{\%SpO_2}{100}\right) \times \left(1 - \frac{\%HbA1c}{100}\right) \times (c_{HbB} + c_{HbO} + c_{HbA1c}) \quad (14)$$

Now replacing the parameters in (8) from (11), (12), (13) and (14) we get

$$R = \frac{\epsilon_{HbB}(\lambda_1) \times (1 - SpO_2) \times (1 - HbA1c) + \epsilon_{HbO}(\lambda_1) \times SpO_2 \times (1 - HbA1c) + \epsilon_{HbA1c}(\lambda_1) \times HbA1c}{\epsilon_{HbB}(\lambda_2) \times (1 - SpO_2) \times (1 - HbA1c) + \epsilon_{HbO}(\lambda_2) \times SpO_2 \times (1 - HbA1c) + \epsilon_{HbA1c}(\lambda_2) \times HbA1c} \quad (15)$$

where  $HbA1c = (\%HbA1c)/100$ ,  $SpO_2 = (\%SpO_2)/100$

Now the (15) can be rewritten as

$$R = \frac{(\epsilon_{HbB} + SpO_2 \times (\epsilon_{HbO} - \epsilon_{HbB})) + HbA1c \times (\epsilon_{HbA1c} - \epsilon_{HbB} - SpO_2 \times (\epsilon_{HbO} - \epsilon_{HbB}))}{(\epsilon_{HbB} + SpO_2 \times (\epsilon_{HbO} - \epsilon_{HbB})) + HbA1c \times (\epsilon_{HbA1c} - \epsilon_{HbB} - SpO_2 \times (\epsilon_{HbO} - \epsilon_{HbB}))} \quad (16)$$

Now from the definition of ratio **R** (8) we can state from (1) that

$$R = \frac{\delta A_{\lambda_1}}{\delta A_{\lambda_2}} = \frac{\delta \left[ -\log \frac{I}{I_0} \right]_{\lambda_1}}{\delta \left[ -\log \frac{I}{I_0} \right]_{\lambda_2}} = \frac{\left[ \log \frac{I_0(d_2)}{I(d_2)} - \log \frac{I_0(d_1)}{I(d_1)} \right]_{\lambda_1}}{\left[ \log \frac{I_0(d_2)}{I(d_2)} - \log \frac{I_0(d_1)}{I(d_1)} \right]_{\lambda_2}} = \frac{\left[ \log \frac{I(d_1)}{I(d_2)} \right]_{\lambda_1}}{\left[ \log \frac{I(d_1)}{I(d_2)} \right]_{\lambda_2}} \quad (17)$$

So, from this equation we can see that the sensor input intensities can be directly used to calculate the ratio. So, we can say,

$$R_1 = \frac{\delta A_{\lambda_2}}{\delta A_{\lambda_3}} = \frac{\left[ \log \frac{I(d_1)}{I(d_2)} \right]_{\lambda_2}}{\left[ \log \frac{I(d_1)}{I(d_2)} \right]_{\lambda_3}} \quad (18)$$

$$R_2 = \frac{\delta A_{\lambda_1}}{\delta A_{\lambda_3}} = \frac{\left[ \log \frac{I(d_1)}{I(d_2)} \right]_{\lambda_1}}{\left[ \log \frac{I(d_1)}{I(d_2)} \right]_{\lambda_3}} \quad (19)$$

Note that HbA1c and SpO2 can be obtained by solving the simultaneous equations of **R<sub>1</sub>** and **R<sub>2</sub>**, and the values of molar absorption coefficients are required.

Solving the simultaneous equations (18) and (19) leads to the equations for calculating HbA1c and SpO2 values,

$$\%HbA1c = \frac{C_1 R_1 + C_2 R_2 + C_3}{C_4 R_1 + C_5 R_2 + C_6} \times 100\% \quad (20)$$

$$\%SpO_2 = \frac{C_7 R_1 + C_8 R_2 + C_9}{C_{10} R_1 + C_{11} R_2 + C_{12}} \times 100\% \quad (21)$$

## 1.2 The experimental setup

The molar absorption coefficient of equation can be determined after setting up a sophisticated experimental setup in a controlled room environment, which is collected from [28]. In [28], the authors show the experimental setup to measure the molar absorption coefficient for Hb and HbO2 for near-IR (NIR) wavelengths. And after obtaining control glycohemoglobin solutions, the molar absorption coefficient can be estimated by sets of LEDs and PDs of different wavelengths.

## II. Methodology

To estimate the absorption coefficients of different hemoglobin molecules, understanding the dissimilarities among molecular structures is important. Different structures of hemoglobin molecule result in distinctive characteristic peaks in absorption coefficients, though the shape of absorption spectrum mostly remains the same. In adult humans, the structure of hemoglobin (Hemoglobin A) consists of four globular protein subunits (denoted as two and two subunits). Each subunit is tightly associated with a Heme group. The protein chain is formed as an alpha-helix structure, which contains a pocket to strongly bind the Heme group.

The Heme group contains Iron (Fe) covalently bound with Nitrogen (N) atoms. These Fe (in Fe2+ state) atoms bind with the oxygen molecule for oxygen transportation. Fig. 1(a) and 1(b) shows the deoxy and oxy-hemoglobin structure, respectively.

Protein glycation is a very common occurrence in human body. But for prolonged exposure of sugar molecules (glucose, fructose and galactose) cause spontaneous binding with hemoglobin. This non-enzymatic reaction occurs between N-end of globin and monosaccharide (i.e. glucose). The higher the sugar level exposes in the blood; the

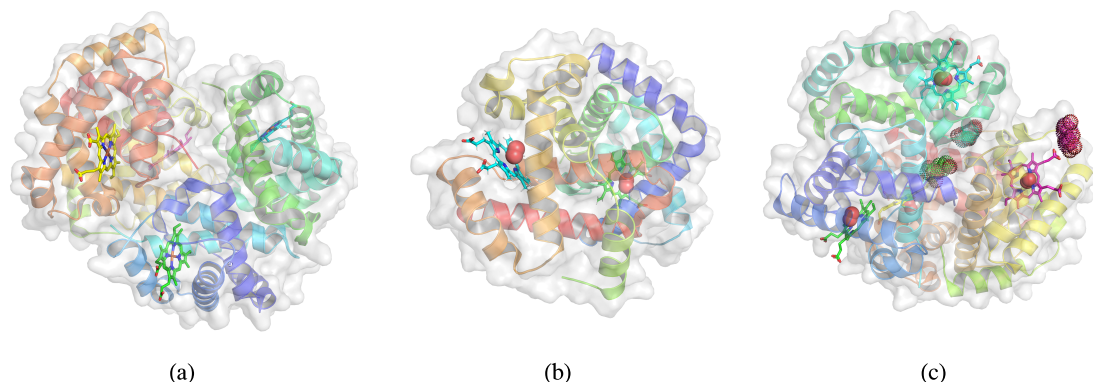


Fig. 1. Molecular structures of (a) Deoxy-hemoglobin, (b) Oxy-hemoglobin and (c) Glycated Hemoglobin. Globular proteins are shown as cartoon and surface. Heme groups are shown as sticks, Oxygen molecules are shown as spheres and, Glucose/Fructose molecules are shown as dotted spheres.

more glycated hemoglobin molecules are produced. Fig. 1(c) shows the glycated hemoglobin structure.

So, it can be clearly seen that the Oxy- and Deoxy-hemoglobin molecules differ in Heme group bond with Oxygen molecule and glycated hemoglobin differs in added monosaccharide. So, their absorption spectrum will be slightly different based on the additional molecules and quantum energy states of the atoms in the hemoglobin molecules.

To estimate the molar absorption coefficient of glycated hemoglobin, a control solution is necessary. There are many control solutions available for HbA1c. Among those Control FD Glycohemoglobin A1c Level-2 (Audit MicroControls) and pure HbA1c control solution (Lee Biosolutions, Inc.) are common. According to [27], these samples are then sandwiched between cover glass and poly prep slides as shown in Fig. 2.

Beer-Lambert law<sup>[27]</sup>, is the linear relationship between absorbance and concentration of an absorbing species. The general Beer-Lambert law is usually written as (1), where A is the measured absorbance, is the molar absorptivity (absorption coefficient), c is the concentration of the compound in solution, and d is the optical path length.

Many compounds absorb ultraviolet (UV) or

visible light. Figure 2 shows a beam of monochromatic radiation of radiant intensity  $I_0$ , directed at a sample solution. Absorption takes place and the beam of radiation leaving the sample has radiant intensity I. The amount of radiation absorbed may be measured in a number of ways:

$$\text{Transmittance, } T = I/I_0 \tag{22}$$

$$\% \text{ Transmittance } \%T = 100T \tag{23}$$

$$\begin{aligned} \text{Absorbance, } A &= -\log T = \log(100/\%T) \\ &= 2 - \log(\%T) \end{aligned} \tag{24}$$

From (24), we can easily calculate absorbance from percentage transmittance data.

The control solutions used contains water as a solvent. Having both the percent transmittance of water and HbA1c solution for the same optical

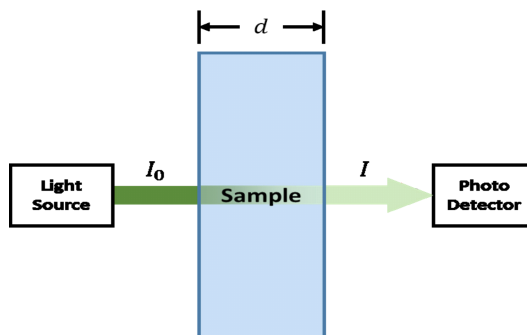


Fig. 2. Experimental Setup for intensity measurement

path length, the absorption of each part can be calculated from the percent Transmittance by using (24) resulting in (25) and (26), respectively.

$$A_{HbA1c_w} = 2 - \log (\% T_{HbA1c_w}) \quad (25)$$

$$A_w = 2 - \log (\% T_w) \quad (26)$$

Then according to Beer Lambert Law, from (1), the absorption coefficient is -

$$C_A = \epsilon c = \frac{A}{d} \quad (27)$$

Now, we can write the full equation of absorption of the solution as,

$$A_{HbA1c_w} = A_w + A_{HbA1c} \quad (28)$$

This equation can be rewritten for the absorption of HbA1c as,

$$A_{HbA1c} = A_{HbA1c_w} - A_w \quad (29)$$

Calculating absorption of a material in the manner, causes scaling error if the transmittance values are normalized. So, now we denote the actual value of absorption of HbA1c as  $A_{HbA1c}^R$  and we can let,

$$A_{HbA1c}^R = k \times A_{HbA1c} \quad (30)$$

If the transmittance values are not normalized, then the value of  $k$  is taken as 1 and for any other normalization factors the coefficient would have a non-unit value. For both of the cases (normalized or actual percent transmittance values) the following equation will satisfy. Now, from (1) we can also replace  $A_{HbA1c}$  from (30) as,

$$A_{HbA1c}^R = k \times \epsilon_{HbA1c}(\lambda) \times c_{HbA1c} \times d \quad (31)$$

And for the same solution used in the experiment, the molar concentration  $c_{HbA1c}$  and the optical path  $d$  remains the same. So we can also

take these two parameters of (31) as a constant. So, we can also write

$$k' = k \times c_{HbA1c} \times d \quad (32)$$

$$A_{HbA1c}^R = k' \times \epsilon_{HbA1c}(\lambda) \quad (33)$$

Now, we can state that, any value of absorption of HbA1c at a certain wavelength is directly proportional to the molar absorption coefficient of HbA1c of that exact wavelength as shown in (34). The (34) can be rewritten for two different wavelengths as (35) shown below,

$$A_{HbA1c}^R \propto \epsilon_{HbA1c}(\lambda) \quad (34)$$

$$\therefore \frac{A_{HbA1c}^R(1)}{A_{HbA1c}^R(2)} = \frac{\epsilon_{HbA1c}(\lambda_1)}{\epsilon_{HbA1c}(\lambda_2)} \quad (35)$$

Now, if any reference molar absorption coefficient value is known for any wavelength, the molar absorption coefficient for the full spectrum can be calculated by the following equation,

$$\epsilon_{HbA1c}(\lambda_2) = \frac{A_{HbA1c}^R(2)}{A_{HbA1c}^R(1)} \times \epsilon_{HbA1c}(\lambda_1) \quad (36)$$

### III. Results and Discussion

According to [29,30], the percent transmittance of HbA1c solution and water can be found for a wavelength range of 300nm to 1100 nm. Fig. 3 illustrates the percent transmittance plots of water and HbA1c in water.

In [31], the authors designed a sensor to estimate glycosylated hemoglobin levels and measured the molar absorption coefficient of HbA1c at two wavelengths of light (535nm and 593nm). They used both 8% and 13% control solution (ControlFD Glycohemoglobin A1c Level-2) to estimate the molar absorption coefficients for those two wavelengths. The molar absorption coefficient values are given below,



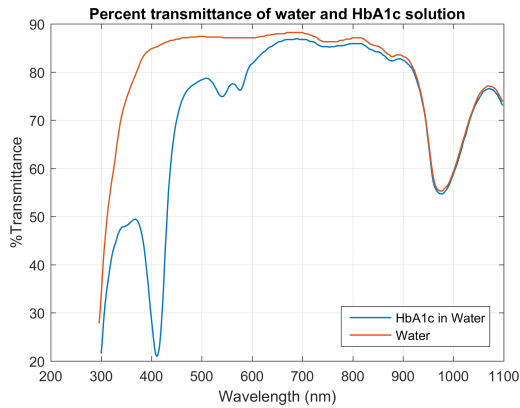


Fig. 3. Percent transmittance of water and HbA1c solution.

$$\epsilon_{HbA1c}^{13\%}(535\text{ nm})=456061 \pm 117823\text{ M}^{-1}\text{ cm}^{-1} \quad (37)$$

$$\epsilon_{HbA1c}^{8\%}(535\text{ nm})=710888 \pm 191458\text{ M}^{-1}\text{ cm}^{-1} \quad (38)$$

$$\epsilon_{HbA1c}^{13\%}(593\text{ nm})=201765 \pm 80037\text{ M}^{-1}\text{ cm}^{-1} \quad (39)$$

$$\epsilon_{HbA1c}^{8\%}(593\text{ nm})=322197 \pm 130060\text{ M}^{-1}\text{ cm}^{-1} \quad (40)$$

These four values of molar absorption

coefficients are used as references to calculate the molar absorption coefficient for 300nm to 1100nm using (36).

Utilizing (29), the absorbance of the HbA1c component is calculated from the total absorbance of the HbA1c solution, where the absorbance of the water for that specific solution is known. After that, the reference HbA1c molar absorption coefficient values (37)-(40) are provided in (36) to calculate the coefficient values for the range of wavelengths.

The estimated molar absorption coefficient for 300nm to 1100nm is depicted in Fig. 4 alongside with the molar absorption coefficient of Oxy- and Deoxy-hemoglobin molecules.

In the range of 300nm to 1100nm we obtained a characteristic peak of molar absorption coefficient of HbA1c at 411nm consisting the mean value of  $5.2049 \times 10^6\text{ M}^{-1}\text{ cm}^{-1}$  and standard deviation of  $1.3969 \times 10^6\text{ M}^{-1}\text{ cm}^{-1}$ .

Other two peaks are detected at 540nm and 576nm having mean of  $5.6383 \times 10^5\text{ M}^{-1}\text{ cm}^{-1}$  and  $4.9683 \times 10^5\text{ M}^{-1}\text{ cm}^{-1}$  and, standard deviation of

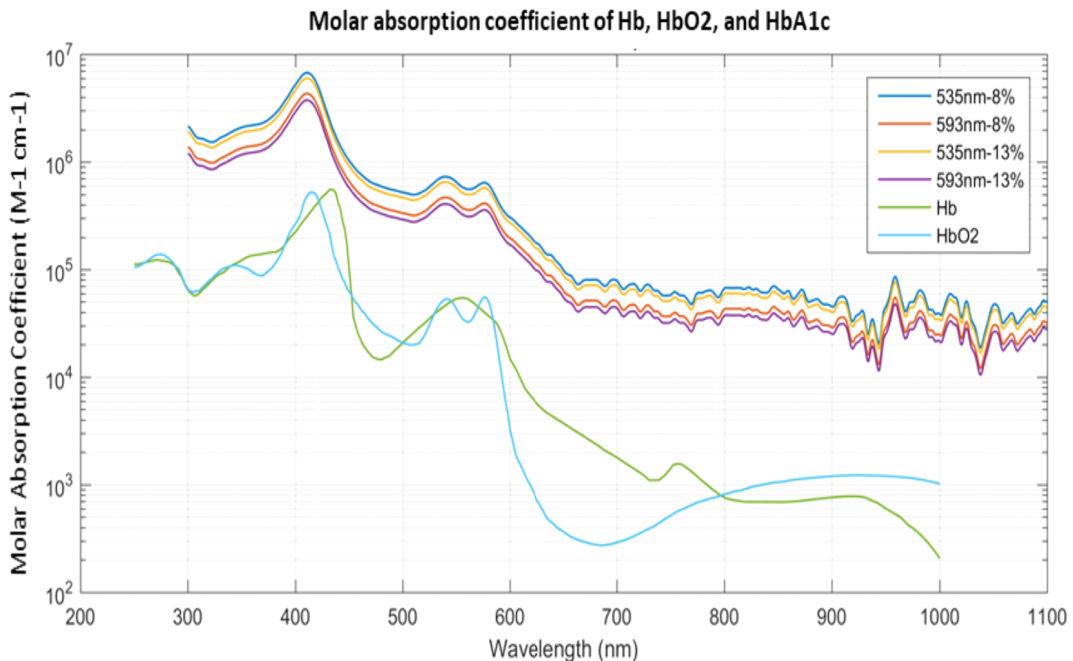


Fig. 4. Molar absorption coefficient of Deoxy-hemoglobin, oxy-hemoglobin and glycated hemoglobin.

$1.5132 \times 10^5 M^{-1} cm^{-1}$  and  $1.3334 \times 10^5 M^{-1} cm^{-1}$  respectively. The peaks found in this experiment (at 411nm, 540nm and, 576nm respectively) are found consistent with [32], [33].

#### IV. Conclusion

In this research, we have focused on the estimation of the molar absorption coefficient of HbA1c. HbA1c is an important marker for diabetes diagnosis. And the molar absorption coefficient is important for non-invasive estimation of the total amount of glycated hemoglobin present in blood stream. We calibrated the molar absorption coefficient of HbA1c and compared with the known peak points of other studies. According to our results we have got the characteristic peaks which are consistent with previous studies, but absorption spectrum needs to be investigated further for wavelengths above 650nm (SW-NIR range). The characteristic peak is found at 411nm. And next two peaks are found at 540nm and 576nm respectively.

#### References

- [1] A. D. Association, "Diagnosis and classification of diabetes mellitus," *Diabetes Care*, vol. 27, no. suppl 1, pp. s5 -s10, Jan. 2004, doi: 10.2337/diacare.27.2007.S5.
- [2] WHO, *Diabetes (2020)*, access date (02, 13, 2020), <https://www.who.int/news-room/fact-sheets/detail/diabetes>.
- [3] S. Kobayashi and Q. Liang, "Autophagy and mitophagy in diabetic cardiomyopathy," *Biochim. Biophys. Acta*, vol. 1852, no. 2, pp. 252-261, Feb. 2015, doi: 10.1016/j.bbdis.2014.05.020.
- [4] V. Bansal, J. Kalita, and U. K. Misra, "Diabetic neuropathy," *Postgrad. Med. J.*, vol. 82, no. 964, pp. 95-100, Feb. 2006, doi: 10.1136/pgmj.2005.036137.
- [5] E. J. Duh, J. K. Sun, and A. W. Stitt, "Diabetic retinopathy: Current understanding, mechanisms, and treatment strategies," *JCI Insight*, vol. 2, no. 14, doi: 10.1172/jci.insight.93751.
- [6] M. D. Mohammed S. Ahmed, *Respiratory infections in diabetes: Reviewing the risks and challenges* (2008), access date (02, 13, 2020) <https://www.patientcareonline.com/respiratory-infections-diabetes-reviewing-risks-and-challenges>.
- [7] J. A. Suaya, D. F. Eisenberg, C. Fang, and L. G. Miller, "Skin and soft tissue infections and associated complications among commercially insured patients aged 0 - 64 years with and without diabetes in the U.S.," *PLoS ONE*, vol. 8, no. 4, Apr. 2013, doi: 10.1371/journal.pone.0060057.
- [8] R. Z. Alicic, M. T. Rooney, and K. R. Tuttle, "Diabetic kidney disease," *Clin. J. Am. Soc. Nephrol.*, vol. 12, no. 12, pp. 2032-2045, Dec. 2017, doi: 10.2215/CJN.11491116.
- [9] S. Chatterjee and A. Mudher, "Alzheimer's disease and type 2 diabetes: A critical assessment of the shared pathological traits," *Front. Neurosci.*, vol. 12, 2018, doi: 10.3389/fnins.2018.00383.
- [10] M. K. Rhee, et al., "Random plasma glucose predicts the diagnosis of diabetes," *PLoS ONE*, vol. 14, no. 7, Jul. 2019, doi: 10.1371/journal.pone.0219964.
- [11] W. Aekplakorn, et al., "Detecting prediabetes and diabetes: Agreement between fasting plasma glucose and oral glucose tolerance test in thai adults," *J. Diabetes Res.*, vol. 2015, p. 7, 2015.
- [12] M. B. Davidson, D. L. Schriger, A. L. Peters, and B. Lorber, "Revisiting the oral glucose tolerance test criterion for the diagnosis of diabetes," *J. Gen. Intern. Med.*, vol. 15, no. 8, pp. 551-555, Aug. 2000, doi: 10.1046/j.1525-1497.2000.08024.x.
- [13] C. Chen, et al., "Recent advances in electrochemical glucose biosensors: a review," *RSC Adv.*, vol. 3, no. 14, pp. 4473-4491, Mar. 2013, doi: 10.1039/C2RA22351A.
- [14] A. J. Bandodkar and J. Wang, "Non-invasive



- wearable electrochemical sensors: a review,” *Trends Biotechnol.*, vol. 32, no. 7, pp. 363-371, Jul. 2014, doi: 10.1016/j.tibtech.2014.04.005.
- [15] D. G. Jung, D. Jung, and S. H. Kong, “A lab-on-a-chip-based non-invasive optical sensor for measuring glucose in saliva,” *Sensors*, vol. 17, no. 11, Nov. 2017, doi: 10.3390/s17112607.
- [16] M. A. Arnold and G. W. Small, “Noninvasive glucose sensing,” *Anal. Chem.*, vol. 77, no. 17, pp. 5429-5439, Sep. 2005, doi: 10.1021/ac050429e.
- [17] C. Weykamp, “HbA1c: a review of analytical and clinical aspects,” *Ann. Lab. Med.*, vol. 33, no. 6, pp. 393-400, Nov. 2013, doi: 10.3343/alm.2013.33.6.393.
- [18] A. D. Association, “Executive summary: Standards of medical care in diabetes—2010,” *Diabetes Care*, vol. 33, no. Supplement 1, pp. S4-S10, Jan. 2010, doi: 10.2337/dc10-S004.
- [19] J. Allen, “Photoplethysmography and its application in clinical physiological measurement,” *Physiol. Meas.*, vol. 28, no. 3, pp. R1-39, 2007, <https://doi.org/10.1088/0967-3334/28/3/R01>.
- [20] M. Kim, et al., “Noise-Robust algorithm for PPG signal measurement,” *J. KICS*, vol. 38C, no. 12, Dec. 2013.
- [21] A. Temko, “Accurate heart rate monitoring during physical exercises using PPG,” *IEEE Trans. Biomed. Eng.*, vol. 64, no. 9, pp. 2016-2024, Sep. 2017, doi: 10.1109/TBME.2017.2676243.
- [22] H. Chang, et al., “A method for respiration rate detection in wrist PPG signal using holo-hilbert spectrum,” *IEEE Sensors J.*, vol. 18, no. 18, pp. 7560-7569, Sep. 2018, doi: 10.1109/JSEN.2018.2855974.
- [23] K. Budidha, V. Rybynok, and P. A. Kyriacou, “Design and development of a modular, multichannel photoplethysmography system,” *IEEE Trans. Instrumentation and Meas.*, vol. 67, no. 8, pp. 1954-1965, Aug. 2018, doi: 10.1109/TIM.2018.2810643.
- [24] P. P. Banik, S. Hossain, T.-H. Kwon, H. Kim, and K.-D Kim, “Development of a wearable reflection-type pulse oximeter system to acquire clean PPG signals and measure pulse rate and SpO<sub>2</sub> with and without finger motion,” *Electronics*, vol. 9, no. 11, Nov. 2020.
- [25] S. Hossain and K.-D. Kim, “Estimation of molar absorption coefficients of HbA1c in near UV-Vis-SW NIR light spectrum,” in *Proc. KICS Fall Conf.*, Nov. 2020.
- [26] S. Hossain, S. S. Gupta, T.-H. Kwon, and K.-D. Kim, “Derivation and validation of gray-box models to estimate non-invasive in-vivo percentage glycated hemoglobin using digital volume pulse waveform,” *Scientific Reports*, Nature Research, 2021. (Accepted, will be published)
- [27] Wikipedia, *Beer - Lambert law* (2020), access date (01. 10, 2021), [https://en.wikipedia.org/w/index.php?title=Beer%E2%80%93Lambert\\_law](https://en.wikipedia.org/w/index.php?title=Beer%E2%80%93Lambert_law).
- [28] Y. Zhao, L. Qiu, Y. Sun, C. Huang, and T. Li, “Optimal hemoglobin absorption coefficient data set for near-infrared spectroscopy,” *Biomed. Opt. Express*, vol. 8, no. 11, pp. 5151-5159, 2017, doi:10.1364/BOE.8.005151.
- [29] P.-T. Dong, H. Lin, K.-C. Huang, and J.-X. Cheng, “Label-free quantitation of glycated hemoglobin in single red blood cells by transient absorption microscopy and phasor analysis,” *Sci. Adv.*, vol. 5, no. 5, p. eaav0561, May 2019, doi: 10.1126/sciadv.aav0561.
- [30] P.-T. Dong, H. Lin, and J.-X. Cheng, “Quantitation of glycated hemoglobin in single red blood cells by transient absorption microscopy and phasor analysis (Conference Presentation),” in *Multiphoton Microscopy in the Biomed. Sci. XIX*, vol. 10882, p. 1088225, 2019, doi: 10.1117/12.2511195.
- [31] S. Mandal and M. O. Manasreh, “An in-vitro optical sensor designed to estimate glycated hemoglobin levels,” *Sensors*, vol. 18, no. 4, Apr. 2018, doi: 10.3390/s18041084.
- [32] M. S. Kiran, T. Itoh, K. Yoshida, N.

Kawashima, V. Biju, and M. Ishikawa, "Selective detection of HbA1c using surface enhanced resonance Raman spectroscopy," *Anal. Chem.*, vol. 82, no. 4, pp. 1342-1348, Feb. 2010, doi: 10.1021/ac902364h.

- [33] M. Mallya, R. Shenoy, G. Kodyalamoole, M. Biswas, J. Karumathil, and S. Kamath, "Absorption spectroscopy for the estimation of glycated hemoglobin (HbA1c) for the diagnosis and management of diabetes mellitus: a pilot study," *Photomed. Laser Surg.*, vol. 31, no. 5, pp. 219-224, May 2013, doi: 10.1089/pho.2012.3421

**시팻 호세인 (Shifat Hossain)**



2017년: Khulna University of Engineering and Technology (KUET) 전자공학과 학사  
2021년 2월: 국민대학교 전자공학과 석사  
2021년 3월~현재: 국민대학교 전자공학과 연구원

<관심분야> 디지털통신, 디지털신호처리  
[ORCID:0000-0002-4537-2620]

**권 태 호 (Tae-Ho Kwon)**



2015년 2월: 국민대학교 전자공학과 학사  
2018년 2월: 국민대학교 전자공학과 석사  
2018년 3월~현재: 국민대학교 전자공학과 박사과정

<관심분야> 디지털통신, 디지털신호처리  
[ORCID:0000-0001-6784-5591]

**김 기 두 (Ki-Doo Kim)**



1980년: 서강대학교 전자공학과 학사  
1980년~1985년: 국방과학연구소 연구원  
1988년: 미국 펜실베이니아 주립대학교 전자공학 석사  
1990년: 미국 펜실베이니아 주립대학교 전자공학 박사

1998년~1999년: 미국 UCSD, Visiting Scholar  
1991년~현재: 국민대학교 전자공학부 교수  
<관심분야> 디지털통신, 디지털신호처리  
[ORCID:0000-0001-5052-3844]